Data-driven Fault Diagnosis for PEM Fuel Cell System Using Sensor Pre-Selection Method and Artificial Neural Network Model

Yanqiu Xing, *Student Member*, *IEEE*, Bowen Wang, Zhichao Gong, *Student Member*, *IEEE*, Zhongjun Hou, Fuqiang Xi, Guodong Mou, Qing Du, *Member*, *IEEE*, Fei Gao, *Senior Member*, *IEEE*, Kui Jiao, *Member*, *IEEE*

***Abstract*—Fault diagnosis is a critical process for the reliability and durability of proton exchange membrane fuel cells (PEMFCs). Due to the complexity of internal transport processes inside the PEMFCs, developing an accurate model considering various failure mechanisms is extremely difficult. In this paper, a novel data-driven approach based on sensor pre-selection and artificial neural network (ANN) are proposed. Firstly, the features of sensor data in time-domain and frequency-domain are extracted for sensitivity analysis. The sensors with poor response to the changes of system states are filtered out. Then experimental data monitored by the remaining sensors are utilized to establish the fault diagnosis model by using the ANN model. Levenberg-Marquardt (LM) algorithm, resilient propagation (RP) algorithm, and scaled conjugate gradient (SCG) algorithm are utilized in the neural network training, respectively. The diagnostic results demonstrate that the diagnostic accuracy rate reaches 99.2% and the recall rate reaches 98.3% by the proposed methods. The effectiveness of the proposed method is verified by comparing the diagnostic results in this work and that by support vector machine (SVM) and logistic regression (LR). Besides, the high computational efficiency of the proposed method supports the possibility of online diagnosis. Meanwhile, detecting the faults in the early stage can provide effective guidance for fault tolerant control of the PEMFCs system.**

***Index Terms*—Artificial neural network; Data-driven approach; Fault diagnosis; PEMFCs system; Hydrogen**

I. Introduction

Alternative energy sources have received much attention in the last few decades. Among those alternative energies, hydrogen and fuel cell technology, especially proton exchange membrane fuel cells (PEMFCs), has attracted much interest due to its high-power density, low operating temperature, and fast response. PEMFCs can be applied in many fields, such as stationary power stations and automobile industry [1]. However, reliability and durability are still two main obstacles to its commercialization[2]. Therefore, fault diagnosis of PEMFC has been increasingly acquired attention.

As a nonlinear, dynamic, and time-varying system, a fuel cell system involves the fuel cell stack and multiple auxiliary subsystems including reactant gas supply subsystems, water and heat management subsystems[3]. To accurately detect and identify the faults occurring in the system is not a trivial task. On such basis, a series of studies have been devoted to the PEMFCs fault diagnosis. In the literature, the diagnostic methods are mainly sorted into two categories, i.e., model-based method and data-driven method [4].

In model-based method, residuals between experimental measurements and numerical model outputs could be analyzed for fault identification [5]. Hence, the reliability of the diagnosis results mainly depends on the accuracy of the numerical model. Outbib et al. [5] built an electrical equivalent model, which could be used as a unifying approach to fuel cell systems, for fuel cell flooding detection. Moreover, an interval linear parameter varying (LPV) observer was used to generate an adaptive threshold [6]–[8]. Fault isolation was based on generating a set of residuals with the available sensors and exploit the different sensitivity to the set of considered faults. Liu et al. [9] employed a modified super-twisting sliding mode algorithm to the observe design, based on a simplified nonlinear model. The residual signal was computed online from comparisons between the oxygen excess ratio obtained from the system model and the observe system. Lee et al. [10] used the residual of the heat transfer rate, two coolant flow rates, and one coolant temperature to diagnose the thermal management system of PEMFCs. The faults occurring in the pumps, sensors, and heat exchangers could also be diagnosed by utilizing the residual-based method.

With the performance improvement of modern processors, another branch named data-driven diagnosis has gained increasing attention. The basic principle of the data-driven

Manuscript received xx xx, xx; revised xx x, xx; accepted xx x, xx. Date of publication xx x, xx; date of current version xx x, xx. This work was supported by the National Natural Science Foundation of China (Grant No. 51976138) and the Natural Science Foundation of Tianjin (China) for Distinguished Young Scholars (Grant No. 18JCJQJC46700). Paper no. xxx. (*Corresponding authors: Qing Du, Fei Gao, Kui Jiao.*)

Y. Xing, B. Wang, Z. Gong, Q. Du, and K. Jiao are with the State Key Laboratory of Engines, Tianjin University, 135 Yaguan Road, Tianjin 300350, China (e-mail: xingyanqiu@tju.edu.cn, rabbitbill@tju.edu.cn, gzchao@tju.edu.cn, duqing@tju.edu.cn, kjiao@tju.edu.cn).

Z. Hou is with the Shanghai Hydrogen Propulsion Technology Co., Ltd., Unit 10, BLDG 17, Innovation Park, Lane 56, Antuo Rd. Jiading, Shanghai, China. (e-mail: houzhongjun@shpt.com)

F. Xi, G. Mou are with the Weichai Power Co. Ltd., 197A Fushou St. E, Weifang, 261016, China. (e-mail: xifq@weichai.com, mugd@weichai.com).

F. Gao is with the FEMTO-ST Institute and FCLAB, Univ. Bourgogne Franche-Comté, UTBM, CNRS, Rue Ernest Thierry Mieg, F-90010 Belfort, France. (e-mail: fei.gao@utbm.fr)

diagnosis method is to collect and analyze real-time information from multiple sensor data (historical or not) to detect possible faults. The extraction and selection of correct data features, as well as the identification of system state labels, construct the most critical part of the data-driven method. For feature construction and selection, the diagnosis approach, based on empirical mode decomposition (EMD), relied on the decomposition of PEMFCs output voltage to detect and isolate flooding and drying faults [11]. Steiner et al. [12] and Pahon et al. [13] proposed a multi-scale decomposition feature extraction method based on discrete wavelet transform from the signal-processing domain. This method only used the stack voltage as an input variable. Zhao et al. [14] and Hua et al. [15] also proposed a fault diagnosis method based on multi-sensor signals and principal component analysis (PCA), and a simplified statistic index for fault diagnosis was deduced based on the PCA. The complexity of the system makes more sensors be introduced for better diagnosis performance. Therefore, how to screen the information collected from the most appropriate sensor is the key to realize the diagnosis. To find the optimal sensor set with minimum size, Mao et al. considered both sensor sensitivity and noise resistance. The sensitivity matrix, relating sensor measurements and fuel cell health parameters, was developed via the fuel cell model [16]–[18]. Wavelet transform-based techniques were used to study the sensor consistency during the operation. The sensor sensitivity can be evaluated without PEM fuel cell physical model [19].

Support vector machine (SVM) is the most common algorithm used in data-driven fault diagnosis. Li et al. [20]–[22] combined the directed acyclic graph support vector machine (DAGSVM) with a designed diagnosis rule. To accomplish the diagnosis algorithm in real-time, a highly integrated electronic chip with multiplexing and high-speed computing capabilities was developed. Cao et al. [23] employed ML-SVM for Multi-Label pattern identification. Han et al. [24] proposed a method of the possibilistic fuzzy C-means clustering artificial bee colony support vector machine (PFCM-ABC-SVM), which filtered data with Gaussian noise and reduced the amplitude of characteristic parameters to ±10%. Tian et al. [25] used support vector data description (SVDD) and relevance vector machine (RVM) optimized by the artificial bee colony (ABC) to avoid false alarms in fault diagnosis. Some other methods should be mentioned. Liu et al. proposed a variety of data fusion methods, e.g., a method combing extreme learning machine (ELM) and Dempster-Shafer (D-S) evidence theory [26], and a discrete hidden Markov model (DHMM) fault diagnosis strategy based on K-means clustering [27]. Andújar et al. [28] constructed a diagnosis tree based on expert experience and knowledge. The fault diagnosis of the system was carried out from four aspects, i.e., electrical state, thermal state, fuel state, and stack state. To deal with the time series data of PEMFC system, Gu et al. [29] developed a long short-term memory (LSTM) network model for flooding fault diagnosis, and adopted the auxiliary system statuses as the inputs of the network. Besides, the model-based and data-driven method are combined in some researches. Bharath et al. [30] developed a 3D model of PEMFC based on semi empirical model for membrane drying and flooding faults diagnosis.

As stated in the literature studies, fault diagnosis, especially online fault diagnosis, has been considered as one of the crucial techniques to ensure the safe operation of the fuel cell system. To realize online diagnosis for PEMFCs systems, the computational efficiency of the online diagnosis approach must be considered, since the online algorithms are implemented in embedded systems with limited computational power[22]. On the other hand, when a fault occurs, the abnormal measurement data from PEMFCs system sensors, such as current, voltage, thermocouple, humidification, pressure, and so on, can effectively help us to identify possible fault states [19]. Thus, the use of multiple sensors provides more distinguishable information for specific system faults. However, that leads to a high dimensional dataset during the system operation. As the analysis of high dimensional dataset is complex and time-consuming, a sensor pre-selection method is necessary to maintain the balance between computational time and diagnostic accuracy.

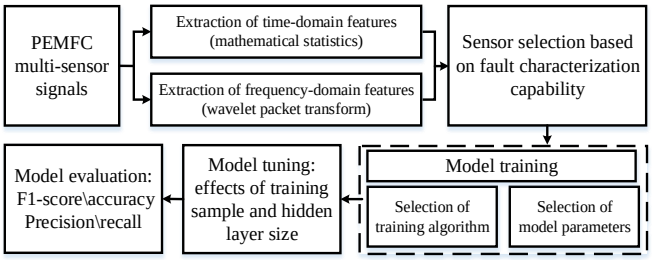

Fig. 1. Flowchart of using multi-sensor data for PEMFC fault diagnosis

In this study, an innovative fault diagnosis strategy for PEMFCs systems based on sensor pre-selection method and artificial neural network (ANN) algorithm is proposed. For sensitivity analysis, features of sensor data in time-domain and frequency-domain are firstly extracted for a selected set of PEMFCs fault conditions. The insensitive data from sensors for a specific fault are removed from the original dataset. Because those data, not only do not improve the diagnosis accuracy but also increase the calculation time. After that, a backpropagation neural network based on the Levenberg-Marquardt training algorithm (LM-BPNN) is trained for fault classification. The influence on diagnosis efficiency of LM-BPNN hidden layer size and training samples distribution is discussed at the end of the paper for practical application. The contributions of this article are as follows:

1) A novel sensor pre-selection method is proposed, which can exclude the useless information and select the optimal sensors for PEMFC system fault diagnosis. The method can apparently reduce the computational complexity of the diagnosis and installation cost of on-board sensors.

2) The proposed sensor selection technique can select the sensor without the use of PEMFC physical model, which is more useful in practical systems. Since the development of high precision and accurate physical model is extremely difficult and time-consuming.

3) The neural network based on Levenberg-Marquart training algorithm has high computational efficiency and diagnostic performance, which is conducive to the realization of online diagnosis.

The remainder of this paper is organized as follows: In Section 2, the proposed method, including sensor selection algorithm and fault classification algorithm, is described. Section 3 introduces the details of the dataset utilized in this study. In Section 4, the effectiveness of the proposed method is verified. From the results, conclusions are listed in Section 5.

TABLE I
TWENTY VARIABLES SELECTED FORM THE PEMFC SYSTEM

Variables	Explanation	Abbreviations
Variables 1	anode outlet pressure #1	AOP1
Variables 2	anode outlet pressure #2	AOP2
Variables 3	cathode outlet pressure #1	COP1
Variables 4	cathode outlet pressure #2	COP2
Variables 5	current	I
Variables 6	anode reactant flow	ARF
Variables 7	anode inlet pressure #1	AIP1
Variables 8	anode inlet pressure #2	AIP2
Variables 9	cathode air inlet flow	CAIF
Variables 10	cathode inlet pressure #1	CIP1
Variables 11	cathode stoichiometry	CS
Variables 12	cathode outlet temperature #2	COT2
Variables 13	cathode inlet temperature #2	CIT2
Variables 14	cathode outlet temperature #1	COT1
Variables 15	cathode inlet temperature #1	CIT1
Variables 16	primary water inlet pressure #2	PWIP2
Variables 17	primary water inlet pressure #1	PWIP1
Variables 18	primary water inlet flow #2	PWIF2
Variables 19	primary water inlet flow #1	PWIF1
Variables 20	water inlet temperature	WIT

II. METHODOLOGIES

In this section, the complete procedure of the proposed method and detailed implementation are presented. The key technologies of PEMFCs system fault detection and diagnosis based on the sensor pre-selection and LM-BPNN are carefully addressed.

Data-preparing is the first step for the data-driven fault diagnosis system, and the data are obtained from historical databases generally. The data utilized in this study were reported by Mao et. al [31]. The dataset contains a total of 206,420 sets of data, and each set contains twenty sensor measurements displayed in Table I (The system consisted of two fuel cell stacks, # expresses the stack number). During the test, two load current modes, constant current and quick fluctuations, were applied to get different system state. With the assistance of post-analysis by electrochemical impedance spectroscopy (EIS), system states can be divided into three categories. The state with the constant load current and without fault was defined as normal, which was represented by label [1 0 0]. The cases with transient load but without fault detected were defined as unknown, which was represented by label [0 1 0]. The state with transient load current and fault was defined as fault, which was represented by label [0 0 1]. The unknown state here can be regarded as the abnormal sensor indication in the practical system. Therefore, the purpose of fault diagnosis in this study is not only to distinguish fuel cell healthy state and fault state, and moreover to separate faulty signals from unknown parts.

A. Framework of Fault Detection and Diagnosis Scheme

The procedure of the proposed fault diagnosis method is shown in Fig.1, and the detailed procedure is as follows:

1) Pretreatment of the data. The data utilized in this study are obtained from historical databases. The original data should be preprocessed firstly. The data set is divided into training set, validation set, and testing set for the subsequent model establishment and verification. To eliminate the influence of singular samples, the above three data sets are normalized by the following formula separately [32]:

$$x_i^* = \frac{x_i - \mathrm{mean}(x_i)}{\mathrm{std}(x_i)} \quad (1)$$

where x_j^* is the normalized variable, j is the dimension of the variable, mean and std are the mean and standard deviation of the j-th dimension, respectively.

2) Sensor pre-selection. Multiple sensors are introduced in the experimental data acquisition. Considering the computational cost and diagnostic accuracy, the original sensors are filtered. The variables with low sensitivity to selected fault conditions are removed from the dataset. This process is carried out through time-frequency analysis of the sensors. The remaining data, recorded by filtered sensors, are used as input variables in the next segment.

3) Establishment of LM-BPNN. The selected sensor with labeled data XL is used to train the entire neural network. Different training algorithms with the Levenberg-Marquardt (LM), resilient propagation (RP), and scaled conjugate gradient (SCG) are compared. The training algorithm with fast convergence speed and better diagnostic performance is selected for better computational efficiency.

4) Verification of the trained LM-BPNN on the testing set. The trained LM-BPNN is utilized to predict the type of each sample in the testing set, and the samples are compared with the real labels to verify the effect of the proposed method.

B. Sensor Pre-Selection Based on Time-Frequency Analysis

The key for the reliable PEM fuel cell fault diagnosis and prognosis is the collection and utilization of sufficient information from the PEM fuel cell system. For this purpose, various sensors, such as current sensor, flow meter, pressure gauge, humidification sensor, etc. were installed in the PEM fuel cell system to collect the system information. As a result, it led to a high-dimensional dataset during the system operation. As stated earlier, to realize online diagnosis for PEMFCs systems, the computational efficiency of the diagnosis approach must be considered. Also, since the data were collected from experiments, it is inevitably contaminated by noise and abnormal data. Therefore, the inclusion of insensitive sensors may not improve the diagnostic results but only increases the computational time. It can be concluded that it is necessary to

further investigate the information in the sensors, and select sensors that are more sensitive to PEM fuel cell system performance variation.

Time-frequency domain analysis is a common method in the field of signal processing, which helps to extract the information hidden behind a large number of seemingly messy data. It is difficult to get the relationship between the sensor and the system state only by the original data recorded by the sensor. In this study, the data collected by each sensor is regarded as a whole. The time-frequency characteristics of each sensor in different system states are calculated respectively. The eigenvalue difference of the same sensor in different system states reveals the sensitivity of the sensor to the system fault condition.

In time-domain analysis, several statistical features are extracted from each sensor variable. Statistics can be used to check the characteristics of the data, including concentration, dispersion and distribution shape of the data. The statistic features extracted from sensor data are listed below:

$$SD = \sqrt{\frac{1}{N}\sum_{i=1}^{N}(S(i) - \text{mean}S(i))^2} \quad (2)$$

$$RMS = \sqrt{\frac{1}{N}\sum_{i=1}^{N}(S(i))^2} \quad (3)$$

$$SK = \frac{\frac{1}{N}\sum_{i=1}^{N}(S(i) - \text{mean}S(i))^3}{SD^3} \quad (4)$$

$$KU = \frac{\frac{1}{N}\sum_{i=1}^{N}(S(i) - \text{mean}S(i))^4}{SD^4} \quad (5)$$

where SD is the standard deviation, RMS is the root mean square, SK is the skewness, KU is the kurtosis, N is the total amount of data for each sensor, S(i) is the value of the data recorded by the i-th sensor, and mean is the mean of the data recorded by the i-th sensor.

In frequency-domain analysis, wavelet packet transform (WPT) is used to decompose the original signal into wavelet packets at different frequency ranges; signals at these frequency ranges are then re-constructed for calculating signal energies. The highest energy is selected for analysis. The generalized energies can be calculated using extracted wavelet packet coefficients below [12]:

$$E^p = \frac{1}{N_p}\sum_{j,k}\left|C_{j,k}^p\right|^2 \quad (6)$$

where p indicates the packet number, $C_{j,k}^p$ are the coefficients contained in the packet p, and N_p is the number of coefficients in the packet p.

In this study, the time-domain analysis results are coupled with the frequency-domain analysis results. The detailed calculation and analysis results are presented in section 3.1. It should be mentioned that the Pearson correlation coefficient (PCC) was also utilized for preliminary screening in previous researches. However, the correlation between variables should obey normal distribution and linear relationships in PCC analysis. Therefore, the application of PCC in the field of fuel cell fault diagnosis needs further consideration.

C. LM-BP Neural Network

ANN has been widely used in industrial fields, such as nonlinear control, system analysis, and data classification [33]. The diagnosis of the fuel cell can be regarded as a supervised classification learning problem. ANN is utilized to accomplish efficient and accurate classification here. As a first-order algorithm, the error backpropagation (EBP) algorithm is the most popular method in training neural networks. However, the EBP algorithm is well known for its low training efficiency.

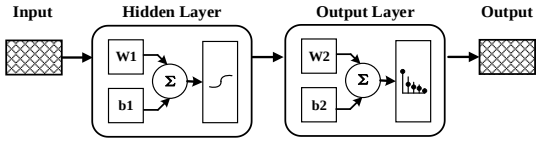

Fig. 2. Pattern recognition neural network

Compared with EBP algorithms possessing constant learning rates, the second-order algorithms can estimate the learning rate in each direction of the gradient using the Hessian matrix, which can significantly increase the training speed. By combining the EBP algorithm and the Newton algorithm, the LM algorithm is ranked as one of the most efficient training algorithms for pattern recognition [34].

1) The Constitution of Artificial Neural Network

The neural network is an operational model composed of a large number of "neurons" and their connections. Each node represents a specific output function called activation function. The sigmoid function is adapted in this study. Each connection between two nodes represents a weighted value, which is called weight, for the signal passing through the connection. Besides, bias matrix is utilized for better data fitting results. The neural network minimizes the loss function by updating the weight matrix and bias matrix to achieve better diagnosis results. Fig.2 shows the general structure of the neural network used for fault diagnosis. In this study, the loss function $L(x^d, \hat{x}^d)$ of the neural network, which is known as the reconstruction error, can be calculated by Eq. (7). Neuronal network hidden layer size n can be calculated according to the Kolmogorov theorem by Eq. (8). The correlation equations are as follows:

$$L(x^d, \hat{x}^d) = \frac{1}{N}\sum_{i=1}^{N}(y_i - h_\theta(x_i))^2 \quad (7)$$

$$n = \sqrt{n_{in} + n_{out} + 1} + a \quad (8)$$

where n_{in} is the number of neurons in the input layer, n_{out} is the number of neurons in the output layer and the a is a constant ($a \in [1,10]$).

The output of the network varies according to the connection mode, weight value, and excitation function of the network. As mentioned previously, the data-driven diagnosis method transforms the problem into supervised classification learning. Therefore, a classifier is selected in the output layer of the neural network. There are two types of classifiers commonly used to deal with multi-category classification problems in machine learning, namely, the SoftMax classifier and the K-Binary classifiers. Their function is to convert linear or nonlinear predictive values into category probabilities. Between two classifiers, the SoftMax classifier is more suitable for the

case of mutual exclusion of classes. In this study, the state of the system is well exclusive (either faulty or healthy). Therefore, the SoftMax classifier is used in the diagnosis of the PEMFCs system.

2) The Levenberg-Marquardt Method

As stated earlier, the training purpose of the neural network is to adjust the weight parameters of the network to minimize the loss function. The optimization method is to find the parameter vector which makes the objective function reach the maximum or minimum value. The traditional BP algorithm uses the gradient descent method to update parameters. The Gauss-Newton method uses the Taylor expansion of objective function to transform the least square problem of a nonlinear function into the least square problem of a linear function in each iteration. The LM can be regarded as a combination of the steepest descent and the Gauss-Newton method. When the current solution is far from the correct one, the algorithm behaves like a steepest descent method: slow but guaranteed to converge. While the current solution is close to the correct solution, it becomes a Gauss-Newton method.

Derived from the gradient descent method and Newton algorithm, the update rule of the LM algorithm is

$$\Delta w = (J^T J + \mu I)^{-1} J^T e \tag{9}$$

where w is the weight vector, I is the identity matrix, and μ is the combination coefficient. The Jacobian matrix J ($P \times M \times N$) and the error vector e ($P \times M \times 1$) are defined as

$$J = \begin{bmatrix} \frac{\partial e_{11}}{\partial w_1} & \frac{\partial e_{11}}{\partial w_2} & \cdots & \frac{\partial e_{11}}{\partial w_N} \\ \frac{\partial e_{12}}{\partial w_1} & \frac{\partial e_{12}}{\partial w_2} & \cdots & \frac{\partial e_{12}}{\partial w_N} \\ \cdots\cdots & \cdots & \cdots & \cdots \\ \frac{\partial e_{PM}}{\partial w_1} & \frac{\partial e_{PM}}{\partial w_2} & \cdots & \frac{\partial e_{PM}}{\partial w_N} \end{bmatrix} \quad e = \begin{bmatrix} e_{11} \\ e_{12} \\ \cdots \\ e_{PM} \end{bmatrix} \tag{10}$$

where P is the number of training patterns, M is the number of outputs, and N is the number of weights. Elements in the error vector e are calculated by

$$e_{pm} = d_{pm} - o_{pm} \tag{11}$$

where d_{pm} and O_{pm} are the desired output and actual output, respectively, at network output m when training pattern p. The LM algorithm terminates when at least one of the following conditions is met [35]:

(i) The magnitude of the gradient of $e^T e$ drops below a threshold ε_1.

(ii) The relative change in the magnitude of δ_p drops below a threshold ε_2.

(iii) The error $e^T e$ drops below a threshold ε_3.

(iv) A maximum number of iterations $k_{\max}$ is completed.

D. Fault Diagnosis Model Performance Measure

To evaluate the diagnostic performance, three evaluation criteria, accuracy, precision, and recall, are proposed. They are essential measurements in the machine learning literature[36]. Taking the binary classification problem as an example, according to the combination of its real category and the prediction category, the sample is divided into four cases: true positives (TP), false positives (FP), true negatives (TN), and false negatives (FN). The TP, FP, TN, and FN denote their corresponding number of samples, respectively.

The precision for fault x is defined as the proportion of faults occurring in the diagnosed ones, herein, it is shown as:

$$Precision = TP / (TP + FP) \tag{12}$$

The recall for fault x is defined as the proportion of faults that diagnosed in the actual faults:

$$Recall = TP / (TP + FN) \tag{13}$$

The accuracy is an additional and complementary indicator, to evaluate the generalization performance globally. It is defined as follows:

$$Accuracy = TP + TN / (TP + TN + FP + FN) \tag{14}$$

Comprehensive consideration of three indicators, the recall is the most important measure, because the purpose of fault diagnosis is to diagnose the fault comprehensively. Also, F1-score is also used for evaluation. It is a measure that combines precision and recall. It represents the balance between the probability that a real event can be detected and the probability that an event has been detected but it does occur. It can be defined as follows:

$$F1score = 2 \times Precision \times Recall / (Precision + Recall) \tag{15}$$

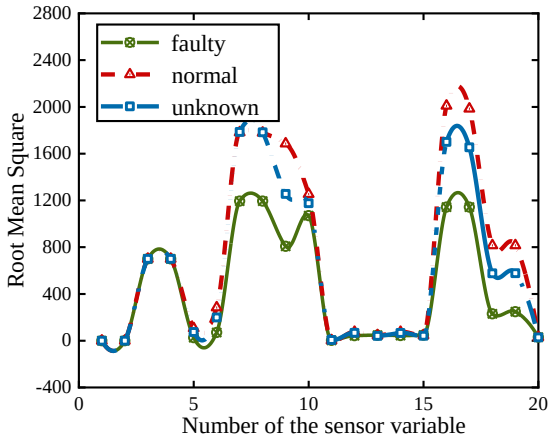

(a)

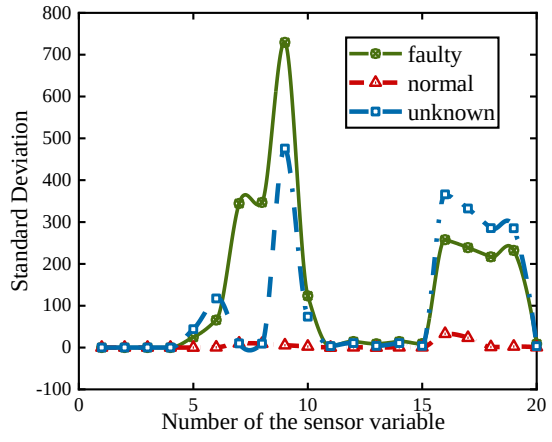

(b)

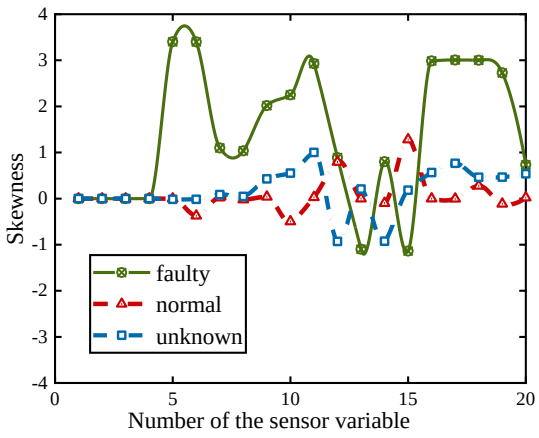

(c)

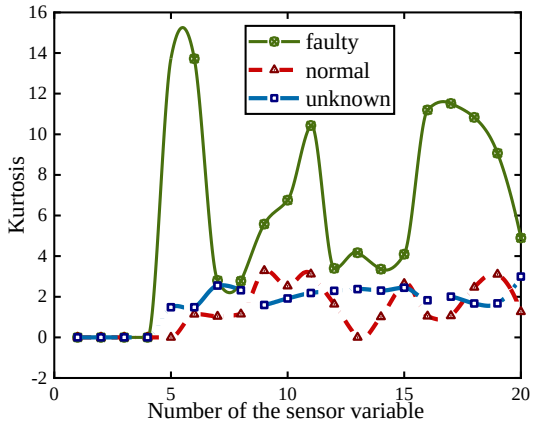

(d)

Fig. 3. Statistical feature of twenty sensor data in the different health status of PEMFC (a) root mean square (b) standard deviation (c) skewness (d) kurtosis

III. Result and Discussion

To verify the effectiveness of the proposed data-based method, the following calculations are carried out. Firstly, the original sensor data are pre-selected with the support of time-frequency analysis; secondly, the LM-BPNNs are trained and verified by using the pre-selected data from the previous step; thirdly, the proposed method is compared with several other methods to demonstrate its effectiveness; finally, the effects on the size of the training set are discussed. It should be mentioned that the proposed method aims to solve the problem of fault diagnosis at the background of PEMFC system with complex multi-sensor and online implementation requirement. Therefore, the methodology can also be applied to fault diagnosis with the same requirements.

A. Effectiveness of Proposed Sensor Pre-Selection Method

To remove the sensor variables that have little correlation with system state variation, the time-frequency characteristics of each sensor in different system states are calculated respectively. In time-domain analysis, the data collected by each sensor is regarded as a whole, and four statistic features are extracted from each sensor using Eq. (2)-(5). As shown in Fig.3, the large the value discrimination of the three states at each sensor, the better the response of the sensor to system changes. In other words, the correlation between the sensor and the system state changes increases with the increase of the separation degree of the four features. It can be seen that the four statistic features of the first four sensors are completely coincident in the three different system states, which indicates the sensor is insensitive to system changes. To quantify the difference value, it is transformed into a binary matrix. When the difference x is too small (for RMS and Std, x<10; for Skewness and Kurtosis, x<1), it is marked as zero; otherwise, it is marked as one. Therefore, the full mark is 12. Tables II-IV show the results of three typical sensor variables. According to the results, the twenty sensors can be divided into three categories. The sensors, with serial numbers of 1, 2, 3, 4, 13, 20, have little relationship with the system state (proportion of score to full marks less than 25%). The sensors, with serial numbers of 5, 7, 8, 11, 12, 14, 15, show a certain degree relationship with system variation (proportion of score to full marks between 25% and 75%). And the response of other sensors to system changes is significant (proportion of score to full marks more than 75%).

In frequency-domain analysis, the wavelet packet transform is utilized for the entire dataset firstly. The purpose of this process is to find the highest energy, which offers better separation ability for further analysis. In Fig.4, it can be seen that packets 1, 3, 7 are appropriate for discrimination and the packet 7 corresponding energy value is the highest one. This is consistent with the results in [12]. After that, the normalized energy at packet 7 of each sensor is calculated, and the results are shown in Fig.5. The analysis method is similar to that in the time domain. The score of the sensors labeled as 1, 2, 3, 4, 11, 13, 20, is zero in frequency-domain analysis, and the results show a high consistency with time-domain analysis. Sensors with a lower score in both time-domain and frequency-domain will be removed. Therefore, the AOP1, AOP2, COP1, COP2, CIT2, and WIT are filtered. The effectiveness of the sensor selection method is further verified in C of section III.

TABLE II
Anode Outlet Pressure #1 Statistical Features Analyses

Anode outlet pressure #1	std	rms	skewness	kurtosis
Faulty-Normal	0	0	0	0
Unknown-Normal	0	0	0	0
Faulty-Unknown	0	0	0	0

TABLE III
Current Statistical Features Analyses

Current	std	rms	skewness	kurtosis
Faulty-Normal	1	1	0	0
Unknown-Normal	1	1	0	0
Faulty-Unknown	1	1	1	1

TABLE IV
Primary Water Inlet Flow #2 Statistical Features Analyses

Primary water inlet flow	std	rms	skewness	kurtosis
Faulty-Normal	1	1	1	1
Unknown-Normal	1	1	0	0
Faulty-Unknown	1	1	1	1

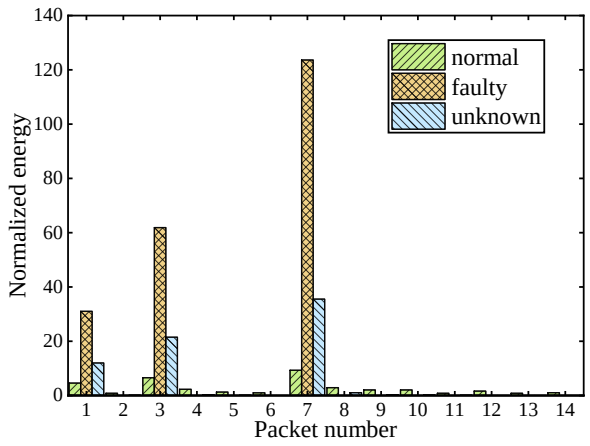

Fig. 4. Energy contained in each packet

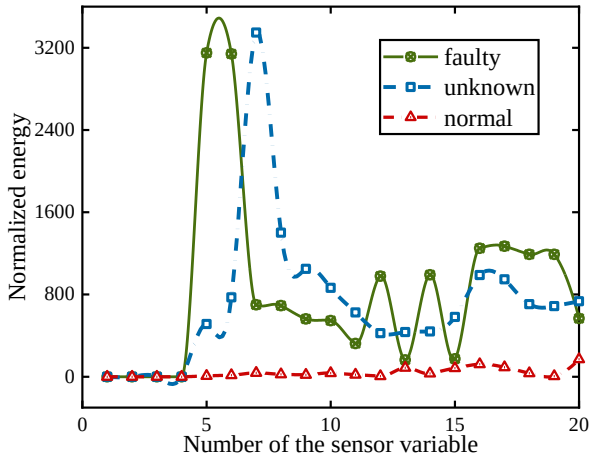

Fig. 5. Wavelet packet decomposition energy characteristics of sensor signal data

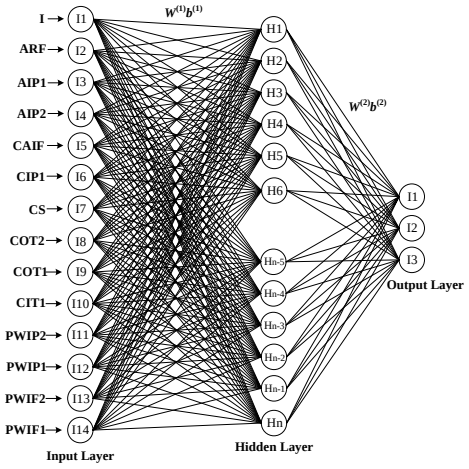

Fig. 6. Neuronal network's final structure

B. *Evaluation of the Training Algorithms*

After sensor selection, the remaining variables are selected for training the neural networks as shown in Fig.6. The pre-selected sensors are used as the input variables of a neural network, and the output variables correspond to three system states. The data is firstly normalized by Eq. (1), then the dataset is randomly selected into training set (60%), validation set (20%), and test set (20%). The training set is used to determine the model parameters; the validation set is employed to tune the model parameters, and the test set is utilized to verify the performance of the model diagnosis. LM algorithm, SCG algorithm, and the RP algorithm, which have been commonly used in supervised learning, are utilized in the training stage, respectively. The purpose of the training algorithm is to adjust the parameters to minimize the loss function. To evaluate parameter performance, the mean-square error (MSE) is chosen as the loss function.

As shown in Fig.7, the LM algorithm has a faster convergence rate and it has begun to converge in the 50th epoch, while SCG and RP have begun to converge in the 150th epoch. In this study, the criteria for stopping iteration are that the loss function is less than 0.001. It can be seen that the LM algorithm stops iteration in the 120th epoch, whereas the SCG and the RP algorithm need over 200 epochs. Moreover, in the process, the training loss of LM is smaller than another algorithm all along. In conclusion, the LM training algorithm converges quickly with smaller training loss, which has considerable practical value in reality.

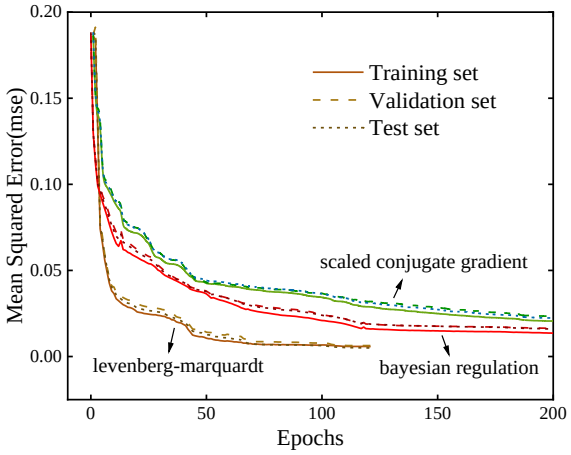

Fig. 7. Learning curves of the different training algorithm: Scaled Conjugate Gradient vs. Bayesian Regulation vs. Levenberg-Marquardt

TABLE V
DIAGNOSTIC EVALUATION OF FOUR CLASSIFICATION ALGORITHMS

Algorithm	SVM	LR	LM-BPNN-all	LM-BPNN
Accuracy (%)	95.57	90.62	95.37	99.18
Precision (%)	99.31	91.29	88.01	99.59
Recall (%)	90.45	89.46	93.87	98.06

C. *Diagnosis Results Compared with the Other Methods*

To validate the performance of the proposed LM-BPNN method, three other methods: SVM, Logistic Regression (LR), and LM-BPNN without sensor pre-selection, are used for comparison. For the sake of convenience, the abbreviation of the proposed method is recorded as LM-BPNN, and the abbreviation of LM-BPNN without sensor selection is recorded as LM-BPNN-all. The hyperparameter of SVM and LR are selected by grid-search for better diagnosis performance. Table VI lists the parameters of the LR; Table VII displays the parameters of the SVM. The parameters of the LM-BPNN-all are the same as the LM-BPNN as shown in Table VIII. The sole diversity between them is whether the sensor is filtered in the

data processing stage. It should be mentioned that the LM-BP neural network in this work was running in the MATLAB R2019a; the SVM and the LR was running in python 3.8.3.

TABLE VI
PARAMETERS OF LOGISTICREGRESSION MODEL

Parameters	Value
'C'	1
class_weight	None
dual	False
fit_intercept	True
intercept_scaling	1
l1_ratio	None
max_iter	100
multi_class	auto
n_jobs	None
penalty	12
random_state	None
solver	lbfgs
tol	0.0001
verbose	0
warm_start	False

TABLE VII
PARAMETERS OF SUPPORT VECTOR MACHINE MODEL

Parameters	Value
'C'	1
break_ties	False
cache_size	200
class_weight	None
coef0	0
decusuib_function_shape	ovr
degree	3
gamma	scale
kernel	rbf
max_iter	-1
probability	False
random_state	None
shrinking	True
tol	0.001
verbose	False

TABLE VIII
PARAMETERS OF SUPPORT VECTOR MACHINE MODEL

Parameters	Value
trainFcn	Levenberg-Marquardt
hiddenLayerSize	10
divideFcn	dividerand
trainRatio	60%
valRatio	20%
testRatio	20%
performFcn	mean squared error
activation functions	sigmoid

The accuracy, precision, and recall in the testing data set of the above four methods are shown in Table V. It can be seen that the proposed LM-BPNN method engenders the best fault diagnosis results, of which the accuracy rate reaches 99.2%, the precision rate reaches 99.5% and the recall rate reaches 98.3%. Due to the large proportion of data in normal state, high accuracy and precision can be obtained by correctly identifying the data in the normal state. However, the most concerned part of fault diagnosis is the fault part. Therefore, as a more concerned evaluation index in fault diagnosis, the high score of the recall reveals the proposed method can deduce most of the system faults.

The diagnosis result of SVM reaches the same level as LM-BPNN in the precision of diagnosis in Table V, but the lower score of the recall means the faulty state and the unknown state cannot be distinguished well in SVM. Meanwhile, as a small sample learning method, its time-cost increases rapidly with the growth of training data samples. It is noteworthy that the LM-BPNN-all uses all the data monitored in the experiment as input variables; its diagnostic performance is not as good as LM-BPNN. It confirms that the proposed sensor selection method is effective; with an optimal sensor set, different fuel cell states can be discriminated with better quality.

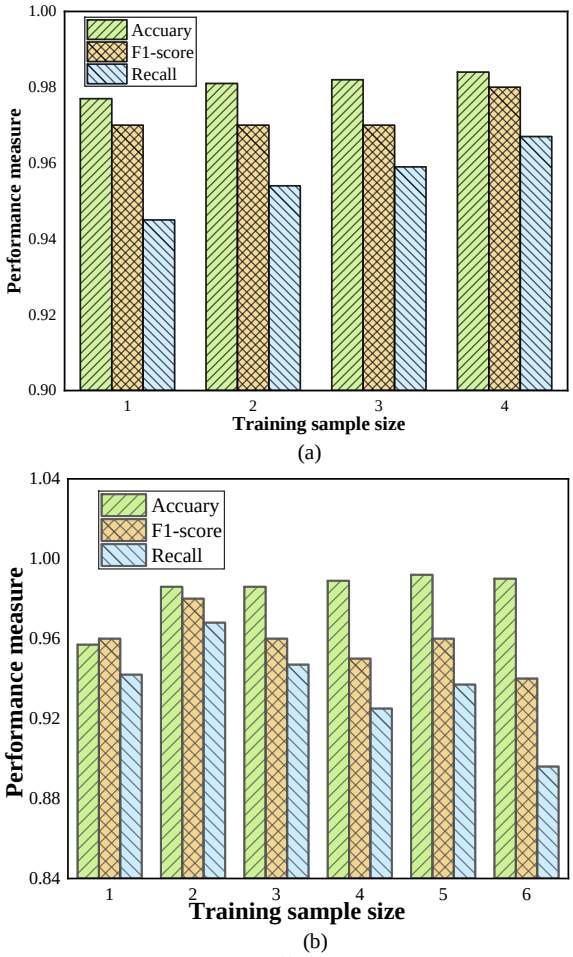

Fig. 8. Fault diagnosis results with different training sample sizes (a) the data proportion of the three system states is fixed (b) only the data of the healthy and unknown are added in the training set

D. *Effects of Training Sample Size*

To explore the relationship between the size of the training set and the fault diagnosis performance when the LM-BPNN methods are applied, comparative experiments using different training set sizes are performed. Fig.8 shows the diagnosis accuracy, recall, and F1-score with different training sample sizes when the LM-BPNN methods are applied. The historical dataset obtained from the EC fuel cell system is 206,400 in total

(normal-171,000, faulty-111,111, unknown-24,260). The data proportion of the three system states in Fig.8 (a) is consistent all the time; while in Fig.8 (b), only the data of healthy and unknown are added in the training set. The number on the horizontal axis represents the percentage of the total dataset.

It can be seen that the accuracy of the diagnosis diminishes with decreasing training samples in Fig.8 (b); the main reason is that the limited training samples cannot provide enough classification information. This reveals that the LM-BPNN based method is suitable for dealing with large-scale training sets. However, the recall score does not appear the same trend as the accuracy; the lowest recall is obtained when all data sets are utilized. In Fig.8 (a), the recall and the accuracy show consistent changes; they increase slightly with the increase of sample size. Therefore, the trends change of diagnostic performance should be caused by data imbalance. Except for collecting enough training samples for better diagnosis results, the data balance also should be noticed in the practical data accumulation. Nevertheless, in practice, the amount of data collected in the faulty condition is far less than the data in the healthy. To solve the imbalance problem thoroughly, the method of modification to the weights of data under different system states in the loss function of the classification model will be adopted in the future study. Furthermore, it is critical whether the class weight equal to the reciprocal of the proportion of the total number to data scales, in different data scales.

IV. Conclusion

As one of the solutions to increase the PEMFCs system reliability and stability, fault diagnosis can provide effective guidance for fault-tolerant control of the system and effectively reduce equipment downtime maintenance. Due to the multi-domain knowledge is included in the PEMFCs model development, the development of an accurate PEMFCs model is extremely difficult. Moreover, some failure mechanisms cannot be modeled accurately. Therefore, this study develops a data-driven diagnostic technique based on LM-BPNN. To alleviate the data explosion from increasing numbers of sensors located on current systems, and achieve a balance between computational time and diagnostic accuracy, the sensor pre-selection method is utilized before diagnosis.

The sensors are filtered through the analysis of time-domain (statistical method) and frequency-domain (wavelet packet transform); the variables with poor response to the changes in system states are removed from the original dataset. Later diagnosis results confirm that the proposed sensor pre-selection method is effective; with an optimal sensor set, different fuel cell states can be discriminated with better quality. The data, obtained from the historical databases and experienced pre-selection, are utilized to train the neural network. According to practical application, a sigmoid function is chosen as the activation function, and the SoftMax classifier is used in the output layer. For the sake of high computational efficiency, the training algorithm, i.e., LM, SCG, and RP, are employed separately. The result reveals that the LM algorithm can converge quickly and with smaller training loss. Furthermore, the comparison with three other frequently-used methods validate the better performance of the LM-BPNN with the pre-selection method. Results demonstrate that with the proposed method, the fault state of the system can be identified quickly and effectively.

In conclusion, the overall results indicate that the optimal sensors can yield reliable system information and reduce unnecessary calculation burden. Besides, the LM-BPNN based method offers the possibility of online diagnosis because of its high computational efficiency. It should be mentioned that this study can be employed in further work, which considers the sensitivity of sensors to system performance changes under different failure modes.

Acknowledgment

Present study is supported by the National Natural Science Foundation of China (Grant No. 51976138) and the Natural Science Foundation of Tianjin (China) for Distinguished Young Scholars (Grant No. 18JCJQJC46700).

References

[1] Z. Li, R. Outbib, S. Giurgea, and D. Hissel, "Fault Diagnosis for PEMFC Systems in Consideration of Dynamic Behaviors and Spatial Inhomogeneity," *IEEE Trans. Energy Convers.*, vol. 34, no. 1, pp. 3–11, 2019, doi: 10.1109/TEC.2018.2824902.

[2] R. Vepa, "Adaptive state estimation of a PEM fuel cell," *IEEE Trans. Energy Convers.*, vol. 27, no. 2, pp. 457–467, 2012, doi: 10.1109/TEC.2012.2190073.

[3] F. D. Bianchi, C. Ocampo-Martinez, C. Kunusch, and R. S. Sánchez-Peña, "Fault-tolerant unfalsified control for PEM fuel cell systems," *IEEE Trans. Energy Convers.*, vol. 30, no. 1, pp. 307–315, 2015, doi: 10.1109/TEC.2014.2351838.

[4] Z. Li, C. Cadet, and R. Outbib, "Diagnosis for pemfc based on magnetic measurements and data-driven approach," *IEEE Trans. Energy Convers.*, vol. 34, no. 2, pp. 964–972, 2019, doi: 10.1109/TEC.2018.2872118.

[5] A. Hernandez, D. Hissel, and R. Outbib, "Modeling and fault diagnosis of a polymer electrolyte fuel cell using electrical equivalent analysis," *IEEE Trans. Energy Convers.*, vol. 25, no. 1, pp. 148–160, 2010, doi: 10.1109/TEC.2009.2016121.

[6] S. De Lira, V. Puig, and J. Quevedo, "LPV model-based fault diagnosis using relative fault sensitivity signature approach in a PEM fuel cell," *IFAC Proc. Vol.*, no. 1, pp. 528–533, 2009, doi: 10.3182/20090630-4-ES-2003.0335.

[7] S. De Lira, V. Puig, J. Quevedo, and A. Husar, "LPV observer design for PEM fuel cell system: Application to fault detection," *J. Power Sources*, vol. 196, no. 9, pp. 4298–4305, 2011, doi: 10.1016/j.jpowsour.2010.11.084.

[8] S. De Lira, V. Puig, and J. Quevedo, "Robust LPV model-based sensor fault diagnosis and estimation for a PEM fuel cell system," *Conf. Control Fault-Tolerant Syst. SysTol'10 - Final Progr. B. Abstr.*, pp. 819–824, 2010, doi: 10.1109/SYSTOL.2010.5676000.

[9] J. Liu, W. Luo, X. Yang, and L. Wu, "Robust Model-Based Fault Diagnosis for PEM Fuel Cell Air-Feed System," *IEEE Trans. Ind. Electron.*, vol. 63, no. 5, pp. 3261–3270, 2016, doi: 10.1109/TIE.2016.2535118.

[10] H. Oh, W. Y. Lee, J. Won, M. Kim, Y. Y. Choi, and S. Bin Han, "Residual-based fault diagnosis for thermal management systems of proton exchange membrane fuel cells," *Appl. Energy*, vol. 277, no. March, p. 115568, 2020, doi: 10.1016/j.apenergy.2020.115568.

[11] C. Damour, M. Benne, B. Grondin-Perez, M. Bessafi, D. Hissel, and J. P. Chabriat, "Polymer electrolyte membrane fuel cell fault diagnosis based on empirical mode decomposition," *J. Power Sources*, vol. 299, pp. 596–603, 2015, doi: 10.1016/j.jpowsour.2015.09.041.

[12] N. Y. Steiner, D. Hissel, P. Moçotéguy, and D. Candusso, "Non intrusive diagnosis of polymer electrolyte fuel cells by wavelet packet

transform," *Int. J. Hydrogen Energy*, vol. 36, no. 1, pp. 740–746, 2011, doi: 10.1016/j.ijhydene.2010.10.033.

[13] E. Pahon *et al.*, "Solid oxide fuel cell fault diagnosis and ageing estimation based on wavelet transform approach," *Int. J. Hydrogen Energy*, vol. 41, no. 31, pp. 13678–13687, 2016, doi: 10.1016/j.ijhydene.2016.06.143.

[14] X. Zhao, L. Xu, J. Li, C. Fang, and M. Ouyang, "Faults diagnosis for PEM fuel cell system based on multi-sensor signals and principle component analysis method," *Int. J. Hydrogen Energy*, vol. 42, no. 29, pp. 18524–18531, 2017, doi: 10.1016/j.ijhydene.2017.04.146.

[15] J. Hua, J. Li, M. Ouyang, L. Lu, and L. Xu, "Proton exchange membrane fuel cell system diagnosis based on the multivariate statistical method," *Int. J. Hydrogen Energy*, vol. 36, no. 16, pp. 9896–9905, 2011, doi: 10.1016/j.ijhydene.2011.05.075.

[16] L. Mao and L. Jackson, "Selection of optimal sensors for predicting performance of polymer electrolyte membrane fuel cell," *J. Power Sources*, vol. 328, pp. 151–160, 2016, doi: 10.1016/j.jpowsour.2016.08.021.

[17] L. Mao, L. Jackson, and B. Davies, "Effectiveness of a Novel Sensor Selection Algorithm in PEM Fuel Cell On-Line Diagnosis," *IEEE Trans. Ind. Electron.*, vol. 65, no. 9, pp. 7301–7310, 2018, doi: 10.1109/TIE.2018.2795558.

[18] L. Mao and L. Jackson, "Effect of sensor set size on polymer electrolyte membrane fuel cell fault diagnosis," *Sensors (Switzerland)*, vol. 18, no. 9, pp. 1–10, 2018, doi: 10.3390/s18092777.

[19] L. Mao, L. Jackson, W. Huang, Z. Li, and B. Davies, "Polymer electrolyte membrane fuel cell fault diagnosis and sensor abnormality identification using sensor selection method," *J. Power Sources*, vol. 447, no. November 2019, p. 227394, 2020, doi: 10.1016/j.jpowsour.2019.227394.

[20] Z. Li, R. Outbib, S. Giurgea, D. Hissel, and Y. Li, "Fault detection and isolation for Polymer Electrolyte Membrane Fuel Cell systems by analyzing cell voltage generated space," *Appl. Energy*, vol. 148, pp. 260–272, 2015, doi: 10.1016/j.apenergy.2015.03.076.

[21] Z. Li *et al.*, "Online implementation of SVM based fault diagnosis strategy for PEMFC systems," *Appl. Energy*, vol. 164, pp. 284–293, 2016, doi: 10.1016/j.apenergy.2015.11.060.

[22] Z. Li, R. Outbib, S. Giurgea, D. Hissel, A. Giraud, and P. Couderc, "Fault diagnosis for fuel cell systems: A data-driven approach using high-precise voltage sensors," *Renew. Energy*, vol. 135, pp. 1435–1444, 2019, doi: 10.1016/j.renene.2018.09.077.

[23] S. Li, H. Cao, and Y. Yang, "Data-driven simultaneous fault diagnosis for solid oxide fuel cell system using multi-label pattern identification," *J. Power Sources*, vol. 378, no. 1, pp. 646–659, 2018, doi: 10.1016/j.jpowsour.2018.01.015.

[24] F. Han, Y. Tian, Q. Zou, and X. Zhang, "Research on the Fault Diagnosis of a Polymer Electrolyte Membrane Fuel Cell System," *Energies*, vol. 13, no. 10, pp. 2531, May. 2020.

[25] Y. Tian, Q. Zou, and J. Han, "Data-driven fault diagnosis for automotive PEMFC systems based on the steady-state identification," *Energies*, vol. 14, no. 7, 2021, doi: 10.3390/en14071918.

[26] J. Liu, Q. Li, W. Chen, Y. Yan, and X. Wang, "A fast fault diagnosis method of the PEMFC system based on extreme learning machine and dempster-shafer evidence theory," *IEEE Trans. Transp. Electrif.*, vol. 5, no. 1, pp. 271–284, 2019, doi: 10.1109/TTE.2018.2886153.

[27] J. Liu, Q. Li, W. Chen, and T. Cao, "A discrete hidden Markov model fault diagnosis strategy based on K-means clustering dedicated to PEM fuel cell systems of tramways," *Int. J. Hydrogen Energy*, vol. 43, no. 27, pp. 12428–12441, 2018, doi: 10.1016/j.ijhydene.2018.04.163.

[28] J. M. Andújar, F. Segura, F. Isorna, and A. J. Calderón, "Comprehensive diagnosis methodology for faults detection and identification, and performance improvement of Air-Cooled Polymer Electrolyte Fuel Cells," *Renew. Sustain. Energy Rev.*, vol. 88, no. October 2016, pp. 193–207, 2018, doi: 10.1016/j.rser.2018.02.038.

[29] X. Gu, Z. Hou, and J. Cai, "Data-based flooding fault diagnosis of proton exchange membrane fuel cell systems using LSTM networks," *Energy AI*, vol. 4, p. 100056, 2021, doi: 10.1016/j.egyai.2021.100056.

[30] K. V. S. Bharath, F. Blaabjerg, A. Haque, and M. A. Khan, "Model-based data driven approach for fault identification in proton exchange membrane fuel cell," *Energies*, vol. 13, no. 12, 2020, doi: 10.3390/en13123144.

[31] L. Mao, L. Jackson, and S. Dunnett, "Fault Diagnosis of Practical Polymer Electrolyte Membrane (PEM) Fuel Cell System with Data-driven Approaches," *Fuel Cells*, vol. 17, no. 2, pp. 247–258, 2017, doi: 10.1002/fuce.201600139.

[32] Z. Zhang, S. Li, Y. Xiao, and Y. Yang, "Intelligent simultaneous fault diagnosis for solid oxide fuel cell system based on deep learning," *Appl. Energy*, vol. 233–234, no. November 2018, pp. 930–942, 2019, doi: 10.1016/j.apenergy.2018.10.113.

[33] B. M. Wilamowski and H. Yu, "Improved computation for levenbergmarquardt training," *IEEE Trans. Neural Networks*, vol. 21, no. 6, pp. 930–937, 2010, doi: 10.1109/TNN.2010.2045657.

[34] N. M. Nawi, A. Khan, and M. Z. Rehman, "A New Levenberg Marquardt based Back Propagation Algorithm Trained with Cuckoo Search," *Procedia Technol.*, vol. 11, no. Iceei, pp. 18–23, 2013, doi: 10.1016/j.protcy.2013.12.157.

[35] M. I. A. Lourakis, "A Brief Description of the Levenberg-Marquardt Algorithm Implemened by levmar The Levenberg-Marquardt Algorithm," pp. 4–9, 2005.

[36] P. Costamagna *et al.*, "A Classification Approach for Model-Based Fault Diagnosis in Power Generation Systems Based on Solid Oxide Fuel Cells," *IEEE Trans. Energy Convers.*, vol. 31, no. 2, pp. 676–687, 2016.